

# Channel-forming Membrane Permeabilization by an Antibacterial Protein, Sapecin

DETERMINATION OF MEMBRANE-BURIED AND OLIGOMERIZATION SURFACES BY NMR\*

Received for publication, July 18, 2003, and in revised form, November 10, 2003  
Published, JBC Papers in Press, November 20, 2003, DOI 10.1074/jbc.M307815200

Koh Takeuchi<sup>‡§</sup>, Hideo Takahashi<sup>¶</sup>, Mariko Sugai<sup>||</sup>, Hideo Iwai<sup>‡\*\*</sup>, Toshiyuki Kohno<sup>||</sup>,  
Kazuhiisa Sekimizu<sup>‡</sup>, Shunji Natori<sup>‡‡</sup>, and Ichio Shimada<sup>‡¶§§</sup>

From the <sup>‡</sup>Graduate School of Pharmaceutical Sciences, The University of Tokyo, Hongo, Bunkyo-ku, Tokyo 113-0033, Japan, <sup>§</sup>Japan Biological Information Research Center, Japan Biological Informatics Consortium, Hatchobori, Chuo-ku, Tokyo, 104-0032, Japan, <sup>¶</sup>Biological Information Research Center, National Institute of Advanced Industrial Science and Technology, Aomi, Koto-ku, Tokyo 135-0064, Japan, <sup>||</sup>Mitsubishi Kagaku Institute of Life Sciences, Minamiooya, Machida, Tokyo 194-8511, Japan, <sup>‡‡</sup>Natori Special Laboratory, Riken, Wako, 351-0198, Japan, and the <sup>\*\*</sup>Department of Chemistry, University of Saskatchewan, Science Place, Saskatoon, SK, S7N 5C9, Canada

**The action mechanism of sapecin, an antibacterial peptide with membrane permeabilization activity, was investigated. The dose dependence of the membrane permeabilization caused by sapecin was sigmoidal, suggesting that sapecin oligomerization leads to the membrane permeabilization. Solution nuclear magnetic resonance analysis of the sapecin-phospholipid vesicle complex revealed the surface buried in the membrane and oligomerization surface on the sapecin molecule. The membrane-buried surface of sapecin was determined by observing the transferred cross-saturation phenomena from the alkyl chains of the phospholipid vesicle to the amide protons of sapecin. The membrane-buried surface contains basic and highly exposed hydrophobic residues, which are suitable for interacting with the acidic bacterial membrane. The oligomerization surface was also identified by comparisons between the results from hydrogen-deuterium exchange experiments and transferred cross-saturation experiments. On the basis of the results from the NMR experiments we built a putative model of sapecin oligomers, which provides insights into the membrane permeabilization caused by insect defensins.**

insect defensins kill a wide range of Gram-positive bacteria, but few Gram-negative bacteria and fungi are sensitive to the peptides (2–5). A patch clamp experiment applied to the *Phormia terranova* defensin A suggested that it forms oligomeric channels in the bacterial membrane (6). K<sup>+</sup> leakage from the forming channel supposedly leads to ATP depletion and respiration inhibition for the bacteria. However, little is known about the structural mechanism of the membrane permeabilization by the defensins.

Sapecin is an insect defensin purified from the culture medium of NIH-Sape-4, an embryonic cell line of *Sarcophaga peregrina* (flesh fly) (7). Sapecin consists of 40 amino acid residues, including three disulfide bonds, which are essential for the antibacterial activity (8). The solution structure of sapecin was solved in methanol by NMR techniques (PDB code 1L4V) (9). The structure revealed that the peptide consists of an N-terminal loop (residues 4–12), an  $\alpha$  helix (residues 15–23), and a two-stranded  $\beta$  sheet (residues 24–31 and 34–40), with three disulfide bridges connecting these structural elements. Sapecin can inhibit the growth of Gram-positive bacteria (*Staphylococcus aureus*) at micromolar concentrations (3) and, furthermore, shows high affinity for an acidic phospholipid, cardiolipin (CL)<sup>1</sup> (3). Thus, CL is considered as the main target molecule of the peptide on the bacterial membrane.

In the present paper, we investigated the interaction between the membrane and sapecin and permeabilization modes of sapecin. Surface plasmon resonance (SPR) analyses revealed the interaction properties of sapecin to the membrane. The dose dependence of the membrane permeabilization suggested that sapecin assumes an oligomeric form in the membrane, leading to the membrane permeabilization. The surface buried in the membrane and oligomerization surface on sapecin was successfully identified by solution NMR techniques along with site-specific amino acid substitutions. Based upon these results, we propose a channel-forming mechanism of sapecin for membrane permeabilization.

## EXPERIMENTAL PROCEDURES

**Expression and Purification of Sapecin**—Sapecin was expressed in *Escherichia coli* by using a ubiquitin fusion protein system as described elsewhere (10). In this system sapecin is fused with the C terminus of

Anti-microbial peptides are widely distributed among organisms and exert their activity by permeabilizing the cell membranes of harmful invaders, such as bacteria. Insect defensins are categorized into a family of anti-microbial peptides, which play an essential role in the insect defense system. The insect defensins are composed of 36–51 amino acid residues. The sequence similarities among the insect defensins range from 58 to 95% (1). All of the insect defensins have six conserved cysteine residues involved in three disulfide bridges. When the six cysteine residues are labeled as I–VI, in order from the N to C terminus, the insect defensins share the disulfide connectives of I–IV, II–V, and III–VI. As for the antibacterial selectivity, the

\* This work was supported by a grant from the Japan New Energy and Industrial Technology Development Organization and the National Project on Protein Structural and Functional Analyses from the Ministry of Education, Culture, Sports, Science, and Technology of Japan. The costs of publication of this article were defrayed in part by the payment of page charges. This article must therefore be hereby marked "advertisement" in accordance with 18 U.S.C. Section 1734 solely to indicate this fact.

§§ To whom correspondence should be addressed. Tel. and Fax: 81-3-3815-6540; E-mail: shimada@iw-nmr.f.u-tokyo.ac.jp.

<sup>1</sup> The abbreviations used are: CL, cardiolipin; TCS, transferred cross-saturation; H-D exchange, hydrogen-deuterium exchange; SPR, surface plasmon resonance; HSQC, heteronuclear single quantum coherence; PC, phosphatidylcholine; HPLC, high performance liquid chromatography; MLV, multilamellar vesicle.

*Saccharomyces cerevisiae* ubiquitin, containing a decahistidine tag at its N terminus. The gene encoding sapecin as the ubiquitin fusion protein was subcloned into pET24d using the NcoI and SalI restriction sites. *E. coli* BL21 (DE3) cells were transfected with the expression construct and grown in either LB media or M9 minimal media enriched with the desired stable isotopes for later NMR experiments.

The expressed ubiquitin-sapecin fusion protein was purified by nickel nitrilotriacetic acid-agarose affinity chromatography, cleaved by recombinant yeast ubiquitin hydrolase, and separated by reverse phase HPLC. The amino acid sequence of sapecin (H<sub>2</sub>N-ATCDLLSGTGINHSACAAHCLLRGNRGGYCNGKAVCVCRN-COOH) was confirmed by an amino acid analysis and a time-of-flight mass spectroscopy measurement.

Because all of the Cys residues in sapecin were fully reduced after the purification, the sapecin was oxidized into the native folding in 50 mM NH<sub>4</sub>Cl, pH 7.8, for 24 h at room temperature (11). The refolded native sapecin was re-purified by the reverse phase HPLC to remove the incorrectly folded products. The proper folding of sapecin was confirmed by the anti-bacterial activity with *S. aureus* and the comparison of the <sup>1</sup>H chemical shifts between the recombinant sapecin and sapecin derived from flesh fly (9). Site-directed mutations were designed and introduced by PCR with the corresponding synthetic primers.

**Preparation of Vesicles**—Phospholipids were dried from a CHCl<sub>3</sub> solution under a N<sub>2</sub> stream, and the residual solvent was completely removed under high vacuum for several hours. The dried lipid film was re-hydrated in a buffer suitable for each experiment by vortexing. The resultant vesicles were multilamellar vesicles (MLVs). To prepare small unilamellar vesicles, the MLV solution was tip-sonicated on ice.

**Analysis of Interaction Using SPR**—The interaction of sapecin with the phospholipid membrane was analyzed by SPR using a BIACORE 1000 equipped with an HPA sensor tip. The running buffer for the determination of the affinity contained 10 mM sodium phosphate, pH 7.0, 100 mM NaCl except for the experiments to analyze the salt concentration dependence on the affinity. In those experiments the NaCl concentration was varied. All experiments were carried out at 25 °C. Immediately after the sensor tips were washed with 40 mM octyl glucoside in water for 5 min at a flow rate of 10 μl/min, the small unilamellar vesicle at a concentration of 2 mM with respect to the phospholipids in the running buffer was injected for 40 min at a flow rate of 2 μl/min. At this stage the HPA surface carries multiple phospholipid layers and/or fused liposomes. To remove these lipid products, a short 15-s pulse of 10 mM NaOH at a flow rate of 100 μl/min was applied several times until a stable base line was obtained. A solution of 0.1 mg/ml bovine serum albumin in running buffer was used to assess the extent of the surface coverage by phospholipids. Only the sensor tips with less than 100 resonance units of bovine serum albumin were used for further experiments. Sapecin solubilized in running buffer was passed over the phospholipid-immobilized cell for 150 s at a flow rate of 50 μl/min. The running buffer was then replaced with sapecin solution to measure the dissociation rate constant of sapecin to the phospholipid layers. After each experiment 10 mM HCl and 10 mM NaOH were sequentially injected for 60 s, each at a flow rate of 10 μl/min, to regenerate the surface. The obtained data were analyzed with the BIAevaluation 2.1 software. For the slow dissociation rate interactions, the association and dissociation rate constants ( $k_a$  and  $k_{dis}$ ) and the equilibrium association constants ( $K_A$ ) were determined by fitting them to the resonance curves for each set of concentrations, assuming a 1:1 (Langmuir) interaction. For the fast dissociation rate interaction ( $k_{dis} > 0.1$  s) only the  $K_A$  were determined by using the sapecin concentration dependence of the equilibrium resonance units.

**Glucose Leakage Experiments**—Glucose-entrapping MLVs were prepared by the previously described method (3). Dried CL (2 μmol) lipid was dispersed by adding 0.1 ml of a 0.3 M glucose solution to obtain the MLVs containing glucose, and then 1 ml of 10 mM phosphate buffer, pH 7.0, containing 130 mM NaCl (buffer A) was added. The resultant MLVs were collected by centrifugation at 10,000 × g for 5 min. The vesicles were washed twice with the same buffer to remove the untrapped glucose and, finally, were resuspended in 200 μl of the buffer.

To test the membrane permeabilization activity of sapecin various concentrations of sapecin dissolved in 10 μl of buffer A were added to 10 μl of the glucose-entrapping MLVs. The mixture was incubated at 25 °C for 30 min, and then the amount of glucose released from the liposomes was measured by the glucose oxidase method using a Glucose B-test kit (Wako Chemical). The amount of glucose corresponding to 100% release was determined by adding 10% Triton X-100 instead of sapecin.

To assess the existence of cooperativity we assumed the following simplest scheme.

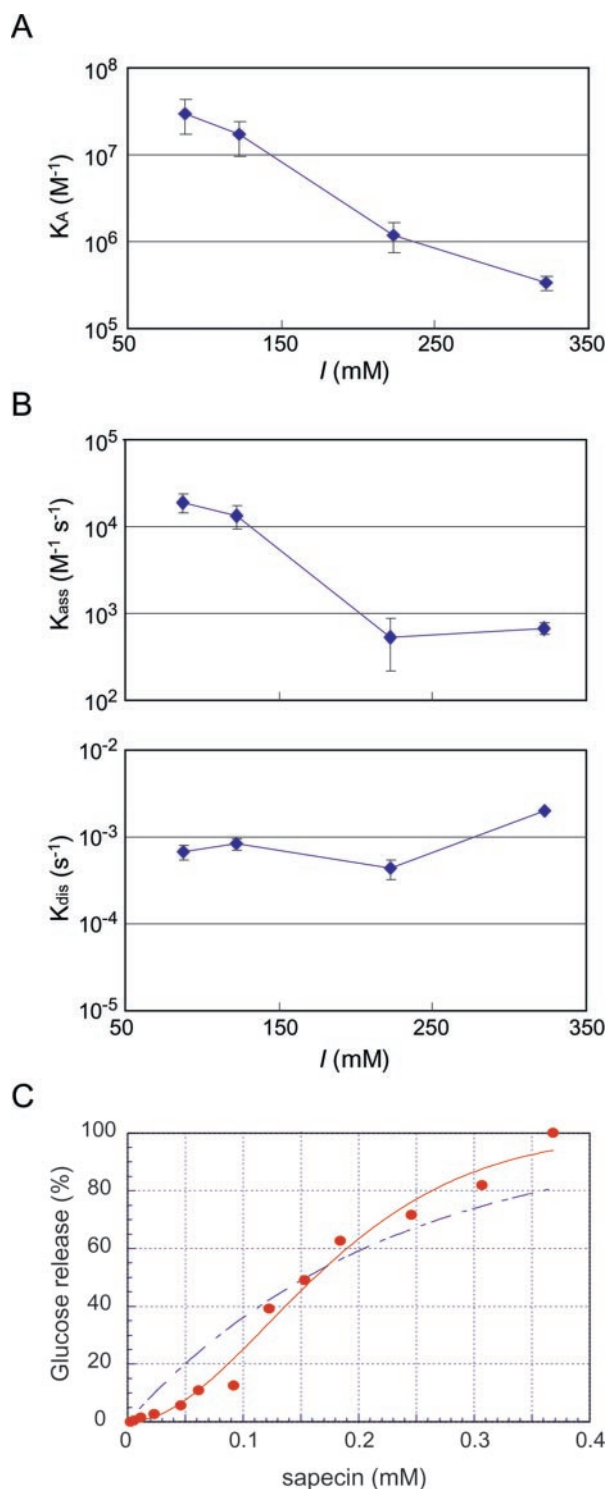


**FIG. 1. Membrane interaction and permeabilization activities of sapecin.** Effects of ionic strength on the equilibrium association constant (A), the association rate constants (B), and the dissociation rate constants (C) of sapecin to a CL monolayer. The binding constants were determined by BIACORE 1000 analyses using a running buffer containing 10 mM sodium phosphate, pH 7.0, and various concentrations of NaCl at 25 °C. Each point is the average of at least two independent measurements, and the error bars represent the S.D. D, amount of glucose leakage from CL vesicles in the presence of sapecin at 25 °C. The curves were least-square fitted by Equation 5 assuming  $n = 1$  (blue dotted line) and 2 (red solid line). In the case of  $n > 1$ , the calculated curves are quite similar to that for the condition of  $n = 2$ .

$$nr_1 \leftrightarrow r_n(\text{pore}) \rightarrow \text{leakage} \quad (\text{Eq. 1})$$

$$r_n = K_n r_1^n \quad (\text{Eq. 2})$$

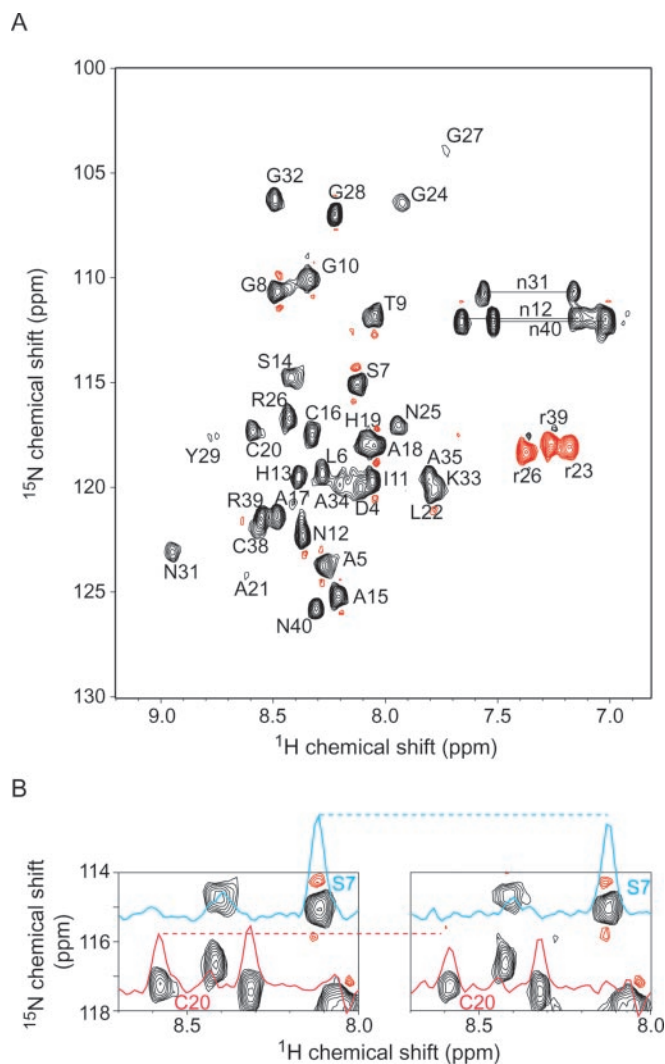


**FIG. 2. Results of TCS experiments.** A, a  $^1\text{H}$ ,  $^{15}\text{N}$  HSQC spectrum of the L5A/V35A mutant of sapeicin, which was in complex with PC vesicles at a concentration of 20 mM with respect to phospholipid. The assignments are indicated with the one-letter amino acid code and residue number. *Upper- and lowercase letters* indicate signals corresponding to backbone and side chain of amino acid groups, respectively. Asn side chain resonances are connected by *lines*. Cross-peaks originating from Arg side chains are folded from upfield in  $\omega 1$  and as a consequence have negative intensity (*red*). B, cross-sections and portions of  $^1\text{H}$ ,  $^{15}\text{N}$  HSQC spectra observed for the labeled sapeicin, which was complexed with the non-labeled PC vesicles without (*left*) and with (*right*) irradiation.

Here,  $r_1$  and  $r_n$  are the densities of the monomeric peptides and  $n$ -meric peptides (pores), respectively.  $K_n$  denotes the oligomerization coefficient. The glucose leakage rate is thought to be proportional to the density of  $n$ -meric peptide,  $r_n$ , and to the concentration of glucose in the liposome. Therefore, we can derive a differential equation for the glucose leakage as Equation 3.

$$-dG(t)/dt = \alpha G(t)r_n \quad (\text{Eq. 3})$$

Here,  $G(t)$  is the amount of glucose in the liposome at time  $t$ , and  $\alpha$  is the leakage rate constant. The total amount of leaked glucose ( $L$ ) after a fixed time ( $T$ ) becomes

$$L = G(0)(1 - \exp(\alpha r_n T)) \quad (\text{Eq. 4})$$

From Equations 1 and 4 we can obtain the normalized leakage  $L$  (%).

$$L(\%) = 100 \times (1 - \exp(\alpha T K_n r_1^n)) \quad (\text{Eq. 5})$$

$$r_1 = r_n - r_{\text{add}} \quad (\text{Eq. 6})$$

$L$  (%) is linear through the origin when  $n = 1$  and becomes sigmoidal

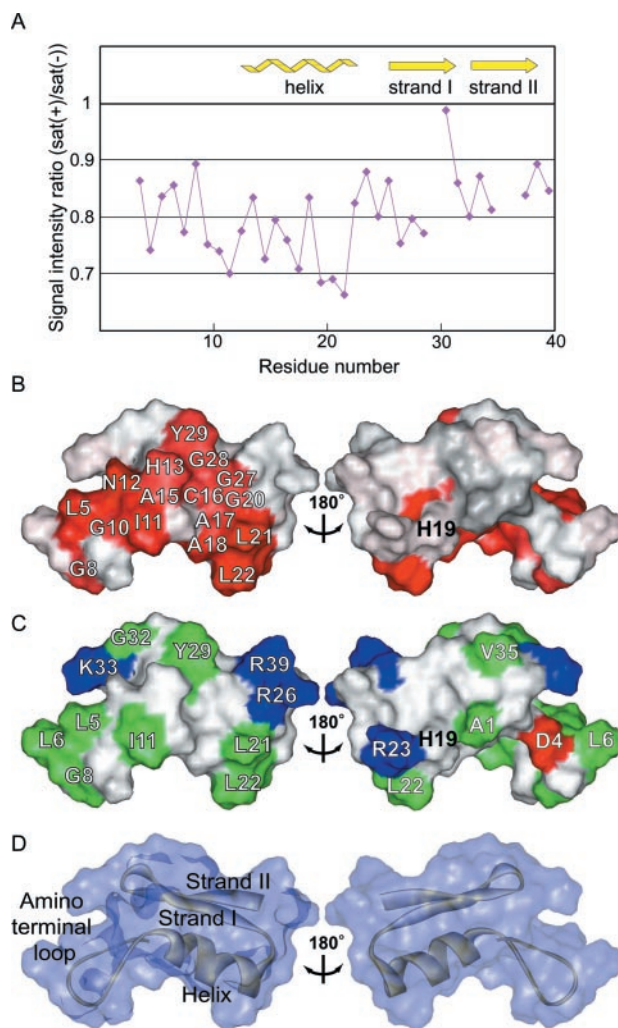


**FIG. 3. Determination of the membrane-insertion site on sapeicin by TCS measurements.** A, signal intensity ratios in the TCS experiment. The L5A/V35A mutant of sapeicin mutant was mixed with PC vesicles at a concentration of 20 mM with respect to phospholipid. The ratios are the average of the results from two independent measurements. The secondary structures of sapeicin are represented by *arrows* for  $\beta$ -sheets and by a *coiled ribbon* for the helix in the plot. B, mapping of the residues affected by the irradiation in the TCS experiments on the solvent-accessible surface of sapeicin molecule. The color ramp from *red* to *white* indicates the signal intensity ratio from 0.7 to 1.0. *Gray* indicates the N-terminal three residues (Ala-1, Thr-2, and Cys-3) and Cys-30, Cys-36, and Val-37, which could not be observed in the HSQC spectra in the TCS experiments. The *left* and *right* figures are  $180^\circ$  rotations about the *vertical axis* relative to each other. C, the distribution of basic (*blue*), acidic (*red*), and solvent-exposed (>30% exposed) hydrophobic residues (*green*) on the solvent-accessible surface of sapeicin molecule. D, ribbon representation of sapeicin molecules with semi-transparent solvent-accessible surface. The view directions of C and D are same as in B.

when  $n > 1$ . The sapeicin concentration dependence of the glucose leakage was fitted by these equations in Figs. 1C and 6A.

**Transferred Cross-saturation (TCS) Experiments**—TCS experiments were carried out as previously described (12–14). All experiments were performed at pH 5.5 on a Bruker Avance 600 spectrometer. A 0.3 mM concentration of  $^2\text{H}$ ,  $^{15}\text{N}$ -labeled L5A/V35A mutant of sapeicin and the MLVs at a concentration of 20 mM with respect to phosphatidylcholine (PC) were dissolved in 10 mM phosphate buffer, pH 5.5, containing 20%  $\text{H}_2\text{O}$ , 80%  $\text{D}_2\text{O}$ . Under these conditions the intensities of the signals from the free sapeicin are reduced to about 70%, as compared with those without the vesicles. Therefore, about 30% of the sapeicin molecules interacted with the vesicles. The salt concentration of the sample was set to 130 mM NaCl. The pulse scheme and the decoupling pulse used for the experiment were the same as described (12). We selectively saturated the vesicles by irradiating resonances from the phospholipid alkyl

TABLE I  
Equilibrium and kinetic binding constants and relative membrane permeabilization activities of sapecin and the mutants for CL membrane

	$k_a^a$ $M^{-1}s^{-1}$	$k_{dis}^a$ $s^{-1}$	$K_A^a$ $M^{-1}$	$R_{K_A}^b$	$R_{ED50}^c$
WT	$1.2 \times 10^4$	$1.1 \times 10^{-3}$	$1.1 \times 10^7$	1.0	1.0
Mutation to the membrane-buried surface					
L5A	$5.9 \times 10^3$	$3.2 \times 10^{-3}$	$1.8 \times 10^6$	0.17	ND
L11A	$1.2 \times 10^4$	$3.5 \times 10^{-3}$	$3.3 \times 10^6$	0.31	0.32
H13A	$5.1 \times 10^3$	$1.6 \times 10^{-3}$	$3.2 \times 10^6$	0.30	0.35
L21A	$1.1 \times 10^4$	$2.3 \times 10^{-3}$	$4.6 \times 10^6$	0.43	0.10
R26A	$2.5 \times 10^3$	$2.3 \times 10^{-3}$	$1.1 \times 10^6$	0.10	ND
Y29W	$8.8 \times 10^3$	$1.6 \times 10^{-3}$	$5.4 \times 10^6$	0.51	0.60
V35A	$5.4 \times 10^3$	$3.0 \times 10^{-3}$	$1.8 \times 10^6$	0.17	ND
R39A	$1.8 \times 10^3$	$1.1 \times 10^{-3}$	$1.7 \times 10^6$	0.16	ND
L5A/V35A	ND	>0.1	$1.2 \times 10^4$	0.01	ND
Mutation to the oligomerization surface					
H19A	$1.1 \times 10^4$	$1.1 \times 10^{-3}$	$1.1 \times 10^7$	0.99	1.8
D4A	$6.8 \times 10^4$	$1.5 \times 10^{-3}$	$4.4 \times 10^7$	4.2	0.75
R23A	$7.2 \times 10^3$	$1.4 \times 10^{-3}$	$5.2 \times 10^6$	0.49	0.32
D4A/R23A	$1.4 \times 10^4$	$0.88 \times 10^{-3}$	$1.6 \times 10^7$	1.5	0.074

<sup>a</sup> Equilibrium and kinetic binding constants of sapecin and the mutants for the CL membrane.

<sup>b</sup> Relative affinity of each mutant to the CL membrane. Each value was calculated from the binding constants, and the value of the wild type sapecin was set to 1.0.

<sup>c</sup> Relative membrane permeabilization activity of each mutant to the CL vesicle. Each value calculated from the concentration causes 50% leakage, and the value of the wild type sapecin was set to 1.0. See "Experimental Procedures" for further details.

chains, using the WURST-2 broadband decoupling scheme. The saturation frequency was set at 0.9 ppm, and the saturation times were set to 1.6 s. Because the saturation scheme was highly selective for the aliphatic proton region, the irradiation of the phospholipid vesicle-sapecin complex affects neither the intensities of the sapecin amide protons nor the water resonance. All spectra were processed with the program nmrPipe.

**Hydrogen-deuterium (H-D) Exchange Experiments**—The lyophilized <sup>15</sup>N-labeled sapecin was dissolved in 450 μl of small unilamellar vesicles containing 1 mM CL and 2 mM PC with respect to phospholipids and was dispersed in 10 mM acetate buffer (pH 3.4, 99.8% D<sub>2</sub>O). The final concentration of sapecin was 0.13 mM. Under these conditions all of the sapecin molecules are complexed with the vesicles, because we could not detect any sapecin resonances in the NMR spectra. After an incubation at 20 °C for 0 (immediately after being dissolved within small unilamellar vesicles), 13, or 30 min, each sample was frozen in liquid N<sub>2</sub> and lyophilized to stop the H-D exchange. During the lyophilization the sample was kept at a temperature of -10 °C to eliminate further exchanges (15, 16). The sample was then re-solubilized in 450 μl of ice-cold C<sup>2</sup>H<sub>5</sub>OH, with added HCl to reduce the pH value, to disrupt the lipid bilayer. The re-solubilized sample was immediately inserted into a pre-shimmed NMR probe, and a heteronuclear single quantum coherence (HSQC) spectrum was collected at 278 K. Control experiments were run in which the lyophilized 0.13 mM <sup>15</sup>N-labeled sapecin was dissolved in 450 μl of 10 mM acetate buffer, pH 3.4, containing 99.8% D<sub>2</sub>O. After an incubation at 20 °C for 0, 5, or 10 min, the H-D exchange was stopped by the same procedure, and the NMR experiment was carried out. All experiments were performed on a Bruker Avance 500 spectrometer.

## RESULTS AND DISCUSSION

**Membrane Interaction Properties of Sapecin**—Sapecin is a basic molecule with a net cationic charge of +3 under physiological conditions. Therefore, like other basic antibacterial peptides, the electrostatic interactions between the acidic phospholipids and basic residues of the peptides are expected to be the driving force of membrane interaction followed by membrane permeabilization. To clarify the participation of the electrostatic interaction, we carried out kinetic analyses of the salt concentration dependence on the interaction between sapecin and the membrane formed with an acidic phospholipid, CL.

Fig. 1A shows the effect of ionic strength on the affinity of sapecin to the CL membrane, as revealed by SPR experiments. As the ionic strength was increased from 88 to 323 mM by adding NaCl (65-300 mM), the affinity was significantly decreased from  $3.0 \pm 1.3 \times 10^7$  to  $3.4 \pm 0.6 \times 10^5 M^{-1}$ . The lower association constant under the high ionic strength conditions was mainly caused by the reduction of the association rate; that is, a 28-fold decrease in the association rate and a 3.0-fold

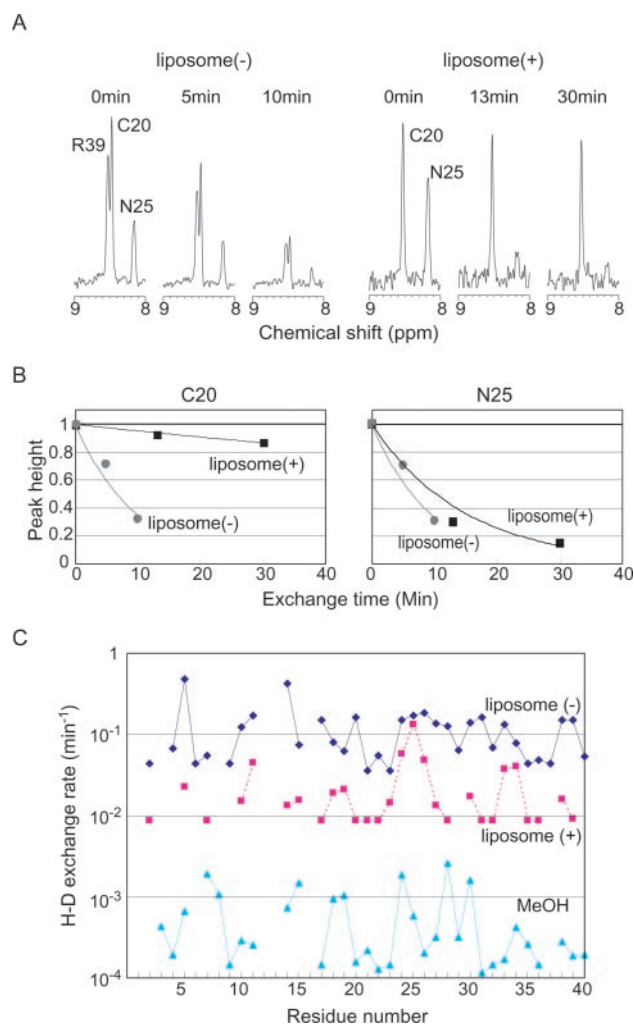
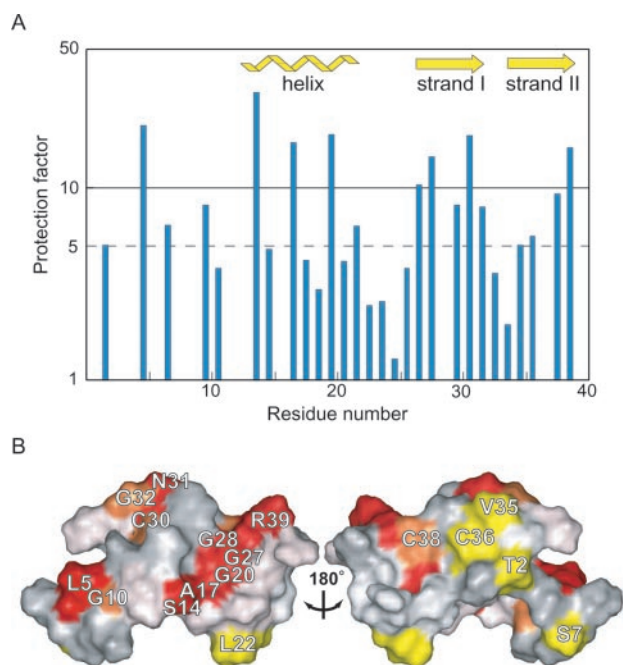


FIG. 4. Results of H-D experiments. A, time dependence of the decay of representative cross-sections of HSQC peaks in free sapecin (left) and vesicle-bound sapecin (right) at pH 3.4 and 20 °C. B, H-D exchange curves of the residues shown in A. Solid lines are the least square fit to determine the first order H-D exchange rates. C, plots of the H-D exchange rates of free (closed diamonds), vesicle-bound (closed squares), and MeOH-solubilized (closed triangles) sapecin as a function of the residue number.



**FIG. 5. Determination of the oligomerization surface on sapecin by H-D exchange experiments.** *A*, protection factors at pH 3.4 and 20 °C as a function of the residue number. The secondary structures of sapecin are represented by arrows for  $\beta$ -sheets and by a coiled ribbon for the helix in the plot. *B*, mapping of the residues with high protection factors in the H-D exchange experiments on the solvent-accessible surface of the sapecin molecule. The color ramp from red to yellow indicates the protection factor from 10 to 5. White indicates the residues with protection factors < 5. Gray indicates the residues that could not be observed in the HSQC spectra in the H-D exchange experiments. The left and right figures are 180° rotations about the vertical axis relative to each other. The view direction is same as in Fig. 3.

increase in the dissociation rate (Fig. 1B). This observation indicates that the electrostatic interaction between the basic residues of sapecin and the phosphate groups of acidic phospholipids serves as the dominant factor in sapecin interaction to the acidic membrane.

**Channel-forming Membrane Permeabilization by Sapecin Oligomer**—The membrane permeabilization activities of sapecin were analyzed by glucose leakage experiments, which use the outward leakage of glucose from glucose-entrapping liposomes as an indicator of membrane permeabilization (3). We precisely analyzed the dose dependence of the glucose leakage caused by sapecin to identify the cooperativity of its membrane permeabilization. The amount of released glucose, which reflects the membrane permeabilization, increased in a sigmoidal manner (Fig. 1C). If the membrane permeabilization by sapecin were not a cooperative process, then the leakage curve would resemble the blue dotted line in Fig. 1C. The observed upper curvature of the glucose leakage at the sapecin concentration around 0.1 mM is strong evidence for the cooperative membrane permeabilization.

The cooperativity in membrane permeabilization has also been described for other anti-bacterial peptides. These peptides are considered to form oligomeric pores in the membrane (17–20). Therefore, we conclude that the oligomerization of sapecin is an essential step in its membrane permeabilization process.

**Determination of the Site Buried in the Membrane on Sapecin**—To identify the site buried in the membrane (membrane-buried site), we performed TCS experiments (12–14). The TCS experiments were carried out under conditions with an excess amount of uniformly  $^2\text{H}$ - and  $^{15}\text{N}$ -labeled sapecin relative to the unlabeled phospholipid vesicle. In the TCS measurements the irradiation of the complex with a frequency corresponding to the

proton resonances of the phospholipid alkyl chains exclusively affects the vesicle, since no aliphatic protons exist in the deuterated sapecin. The irradiation causes the effective saturation of all of the resonance from the phospholipid, due to spin diffusion. The saturation in the phospholipids is not limited within the vesicle but is transferred to the residues at the interface of sapecin through the cross-saturation phenomena. If the reversible exchange of the sapecin and phospholipid vesicle complex exhibits a dissociation rate approximately greater than  $0.1\text{ s}^{-1}$ , then the effect of the cross-saturation is sufficiently observed in the free state of sapecin (21). However, the wild type sapecin slowly dissociates from the membrane. The dissociation rate of sapecin from a membrane that is composed of neutral phospholipid, PC, was  $1.6 \times 10^{-3}\text{ s}^{-1}$ . Therefore, we could not successfully observe the transferred cross-saturation phenomena from the PC vesicles to the wild type sapecin. To achieve the fast dissociation in the interaction of sapecin with membrane we prepared sapecin mutants. Among the mutants, the replacements of Leu-5 and Val-35 with Ala in sapecin satisfactorily accelerated its dissociation rate from the PC membrane ( $k_{\text{diss}} > 0.1\text{ s}^{-1}$ ). Therefore, we utilized the double mutant of sapecin, L5A/V35A, for the subsequent TCS experiments.

The membrane-buried residues on sapecin were identified by a comparison of the peak intensities of the amide groups of free sapecin on  $^1\text{H}$ ,  $^{15}\text{N}$  HSQC spectra with and without irradiation. Fig. 2A shows a  $^1\text{H}$ ,  $^{15}\text{N}$  HSQC spectrum observed for the L5A/V35A mutant of sapecin in the presence of the PC vesicles with the spectral assignments. The chemical shifts observed in the spectrum were completely identical to those from the free molecule, indicating that, under the present measurement conditions only the resonances from the free sapecin were observed in the HSQC spectra of the mixture of sapecin and PC vesicles. The irradiation applied to the NMR sample resulted in selective intensity losses for the free sapecin resonances (Fig. 2B).

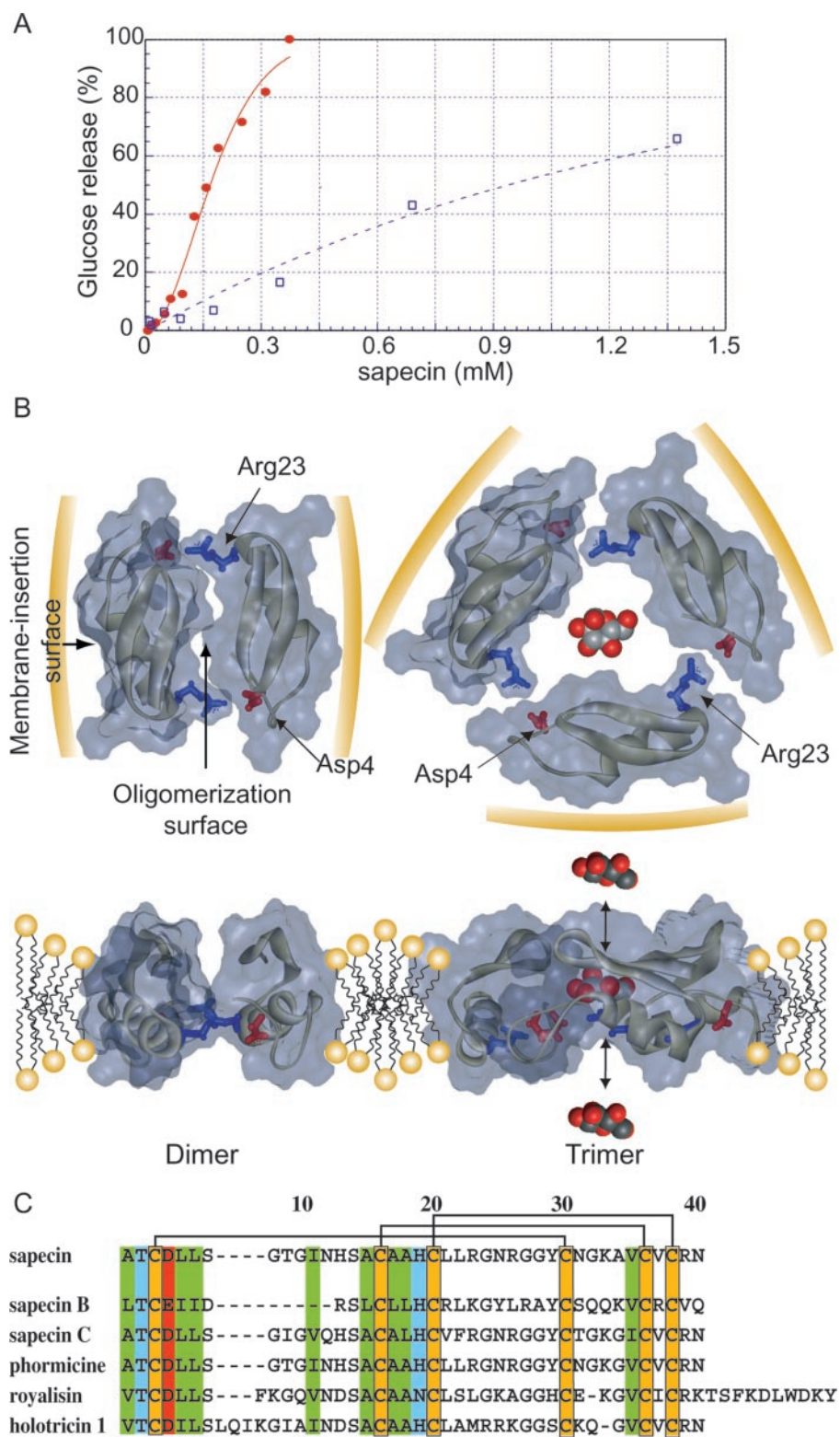
Based on the spectra with and without the irradiation we calculated the reduction ratios of the peak intensities, which are summarized in Fig. 3A. The residues in the helix region were obviously affected by the irradiation. These affected residues formed a contiguous surface on the sapecin structure (Fig. 3B, left). Therefore, we conclude that the membrane-buried site of sapecin to the phospholipid vesicle is composed of the following residues: Leu-5, Gly-8, Gly-10, Ile-11, Asn-12, and His-13 in the amino-terminal loop, Ala-15, Cys-16, Ala-17, Ala-18, Gly-20, Leu-21, and Leu-22 in the  $\alpha$  helix, and Gly-27, Gly-28, and Tyr-29 in the first strand of the  $\beta$  sheet.

Fig. 3C shows the distributions of the basic, acidic, and solvent-exposed-hydrophobic residues on the sapecin surface. Three of the four basic residues, none of the acidic residues, and most of the solvent-exposed hydrophobic residues are on the membrane-buried site of sapecin. Therefore, the surface determined by the TCS experiments is suitable to interact with the acidic phospholipid membrane.

**Introducing Mutations around the Membrane-buried Site of Sapecin**—To confirm the results of the TCS experiments, point mutations were introduced around the membrane-buried site, and then the affinities of the mutants for the CL membrane were measured by SPR. The proton chemical shifts recorded for the sapecin mutants exhibited no drastic change, as compared with that for the wild type. Therefore, all of the mutants prepared in the present study assume a similar fold to that of the wild type. Table I shows the effects of the substitutions on the membrane-interaction activity, as measured by SPR. Mutations within the surface identified by the TCS experiments decreased the affinities to the membrane (L5A, I11A, H13A, L21A, R26A, Y29W, V35A, and R39A), whereas a mutation on the opposite side of the membrane-buried surface (H19A) did

**FIG. 6. Membrane permeabilization mechanism of sapecin.**

**A**, amount of glucose leakage from CL vesicles in the presence of the wild type sapecin (*red closed circles*) and the D4A and R23A doubly mutated sapecin (*blue open squares*) at 25 °C. The curves are least square fits by Equation 5. For the wild type sapecin the curve calculated with the condition of  $n = 2$  (*red solid line*) is shown as a representative for the curves  $n > 1$ . For the doubly mutated sapecin, the curve calculated with the condition of  $n = 1$  (*blue dotted line*) is shown. **B**, putative models of sapecin oligomer. *Left and right figures* show dimer and trimer, respectively. The diagrams show the ribbon representation of sapecin molecules with semi-transparent solvent-accessible surface. Phospholipid membrane is also shown by yellow schematic representation. The upper and lower figures are 90° rotations about the horizontal axis relative to each other. The view of the upper figure is looking down the surface of the membrane with the sapecin oligomer embedded in the bilayer. The side chains of Asp-4 and Arg-23 are shown by a stick representation. In the trimer model a glucose molecule is shown by a Corey-Pauling-Koltun model. **C**, sequence alignment of sapecin with other insect defensins. The residues that are highly conserved within the insect defensins are designated by a colored background. The colors indicate the types of amino acid residues. Hydrophobic, polar, and acidic residues are colored green, cyan, and red, respectively. The connectivity of the cysteine residues is indicated by a line.



not affect on affinity. These results demonstrate that the interface determined by the TCS experiments energetically contributes to the interaction with membrane.

**Determination of the Oligomerization Site on Sapecin**—We also measured the H-D exchange rates for the backbone amide groups of sapecin embedded in bilayer vesicles composed of CL:PC (1:2), with an excess amount of vesicles relative to the peptide. The H-D exchange experiments were performed in  $D_2O$  at 20 °C using uniformly  $^{15}N$ -labeled sapecin and non-labeled vesicles. As a reference we performed the H-D exchange experi-

ment in the same way but without vesicles. After the H-D exchange procedure, the samples were frozen in liquid  $N_2$  and lyophilized to stop the H-D exchange. The samples were then re-solubilized in ice-cold methanol to disrupt the lipid bilayer and immediately inserted into pre-shimmed NMR probes. Furthermore, the H-D exchange rates for the backbone amide groups in methanol were also measured at 4 °C. Based upon the peak intensities of a series of  $^1H$ ,  $^{15}N$  HSQC spectra, we determined the H-D exchange rates for the individual residues of sapecin.

Fig. 4A shows one-dimensional strips of the HSQC spectra of

sapecin, measured as described above. First order H-D exchange rates were calculated from the time dependence of the amide signal reduction in these spectra (Figs. 4, B and C). Considering the fact that the H-D exchange rates in methanol are quite slow, the H-D exchange during the NMR measurement time was almost negligible in the H-D exchange rates obtained from the experiments with and without the vesicles (Fig. 4C). Then the data were converted to the protection factor, which is the ratio of the exchange rate in the free state to that in the vesicle-bound state, for each residue (Fig. 5A).

In the H-D exchange experiments the amide exchange rates for the residues that are located in both the membrane-buried and oligomerization sites are expected to decrease. Therefore, a comparison between the results from the TCS and H-D experiments would reveal the sapecin oligomerization site.

Fig. 5B shows the distribution of residues with protection factors larger than 5. The residues with protection factors larger than 10 are clustered on the membrane-buried surface, which was determined by the TCS experiment. On the other hand, the residues with protection factors between 5 and 10 are mainly distributed on the opposite side of the membrane-buried surface. Therefore, we conclude that the residues on the opposite side of the membrane-buried surface are responsible for the oligomerization of sapecin in the membrane. It should be noted that Asp-4 and Arg-23 are separately located at the both ends of the oligomerization surface (Fig. 3C).

**Mutations of the Sapecin Oligomerization Site**—We introduced mutations of the residues on the oligomerization surface and measured the affinity and permeabilization activities. As shown in Table I, the mutation D4A increases the affinity for membrane but decreases the membrane permeabilization activity. The mutation R23A reduced the affinity to the same level as the mutation Y29W, a mutation within the membrane-buried surface. Interestingly, the membrane permeabilization activity of the R23A mutant was lower than that of Y29W mutant. When Asp-4 and Arg-23 were simultaneously mutated, the membrane permeabilization activity drastically decreased, whereas the affinity to the membrane remained almost the same as that of the wild type. Furthermore, the strong tendency of the cooperative membrane permeabilization, which was observed for the wild type sapecin, significantly declined in the double mutant (Fig. 6A). Therefore, it is likely that Asp-4 and Arg-23 of sapecin are involved in the oligomer formation, leading to the membrane permeabilization.

**Putative Model of Membrane Permeabilization Caused by Sapecin**—The residues Asp-4 and Arg-23 are at opposite ends of the oligomerization site on the sapecin molecule. If putative models of sapecin oligomers are made as shown in Fig. 6B, Asp-4 of one sapecin faces Arg-23 of another sapecin, suggesting that an electrostatic interaction might exist between Asp-4 and Arg-23. This putative model can partially explain the results of the mutation introduced in the oligomerization surface that the double mutant of D4A/R23A exhibits the significant reduction of the membrane permeabilization. However, this does not necessarily mean that the electrostatic interaction is the primary interaction in forming the sapecin oligomers, since the single mutants D4A and R23A still exhibit the membrane permeabilization to a certain extent. Therefore, we conclude that Asp-4 and Arg-23 play a not determinate but key role in the oligomerization, which causes the membrane permeabilization.

In the oligomer larger than a trimer the pore size of the oligomer is large enough for glucose to permeate. On the basis of these results we propose a two-step mechanism for the membrane permeabilization by sapecin. In the first step sapecin interacts with the membrane by using the surface composed of the basic and solvent-exposed hydrophobic residues, and then

it oligomerizes with other sapecin molecules as shown in Fig. 6B, leading to increased membrane permeabilization.

Comparison of the amino acid sequence among insect defensins including sapecin shows the conservation of the amino acids corresponding to Asp-4 and Arg-23 of sapecin. Fig. 6C shows an alignment of the amino acid sequence of sapecin with those of other insect defensins. Asp-4 in sapecin is conserved as an acidic residue within the insect defensin family, except for the *Aeschna* defensin. The conservation of an acidic residue is disadvantageous for the insect defensins to interact with membranes composed of acidic phospholipids. It should be noted that the D4A mutant of sapecin increases the affinity for the CL membrane. However, its conservation seems to be reasonable, since the residue is responsible for sapecin oligomerization and is also essential for the membrane permeabilization activity. As for the *Aeschna* defensin, the time course of its antibacterial activity is known to be slower than those of other insect defensins (22). Considering the lack of the conservation of the acid residue, it is likely that the *Aeschna* defensin utilizes a different bactericidal mechanism from those of the others. The corresponding position of Arg-23 is also highly conserved (59%) within the insect defensins. All of the insect defensins that lack a basic residue at position 23 instead have a basic residue at position 25. Position 25 is close to that of 23 within the sapecin structure (9). Thus, the basic residues at position 25 could complement the absence of the basic residue at position 23.

The oligomerization of insect defensins in the membrane was also described for *P. terranova* defensin A by using monolayer techniques (23). In addition, a patch clamp experiment revealed that *P. terranova* defensin A forms membrane-permeabilizing channels in giant vesicles (6). Considering these results and the high sequence homology within the insect defensins family, the oligomerization on the membrane followed by the permeabilizing channel formation would probably be a common process in the membrane permeabilization by these peptides.

#### REFERENCES

- Bulet, P., Hetru, C., Dimarcq, J. L., and Hoffmann, D. (1999) *Dev. Comp. Immunol.* **23**, 329–344
- Lambert, J., Keppi, E., Dimarcq, J. L., Wicker, C., Reichhart, J. M., Dunbar, B., Lepage, P., Van Dorsselaer, A., Hoffmann, J., Fothergill, J., and Hoffmann, D. (1989) *Proc. Natl. Acad. Sci. U. S. A.* **86**, 262–266
- Matsuyama, K., and Natori, S. (1990) *J. Biochem.* **108**, 128–132
- Lee, S. Y., Moon, H. J., Kawabata, S., Kurata, S., Natori, S., and Lee, B. L. (1995) *Biol. Pharm. Bull.* **18**, 457–459
- Fujiwara, S., Imai, J., Fujiwara, M., Yaeshima, T., Kawashima, T., and Kobayashi, K. (1990) *J. Biol. Chem.* **265**, 11333–11337
- Cociancich, S., Ghazi, A., Hetru, C., Hoffmann, J. A., and Letellier, L. (1993) *J. Biol. Chem.* **268**, 19239–19245
- Matsuyama, K., and Natori, S. (1988) *J. Biol. Chem.* **263**, 17112–17116
- Kuzuhara, T., Nakajima, Y., Matsuyama, K., and Natori, S. (1990) *J. Biochem.* **107**, 514–518
- Hanzawa, H., Shimada, I., Kuzuhara, T., Komano, H., Kohda, D., Inagaki, F., Natori, S., and Arata, Y. (1990) *FEBS Lett.* **269**, 413–420
- Kohno, T., Kusunoki, H., Sato, K., and Wakamatsu, K. (1998) *J. Biomol. NMR* **12**, 109–121
- Kim, J. I., Iwai, H., Kurata, S., Takahashi, M., Masuda, K., Shimada, I., Natori, S., Arata, Y., and Sato, K. (1994) *FEBS Lett.* **342**, 189–192
- Takahashi, H., Nakanishi, T., Kami, K., Arata, Y., and Shimada, I. (2000) *Nat. Struct. Biol.* **7**, 220–223
- Nishida, N., Sumikawa, H., Sakakura, M., Shimba, N., Takahashi, H., Terasawa, H., Suzuki, E. I., and Shimada, I. (2003) *Nat. Struct. Biol.* **10**, 53–58
- Nakanishi, T., Miyazawa, M., Sakakura, M., Terasawa, H., Takahashi, H., and Shimada, I. (2002) *J. Mol. Biol.* **318**, 245–249
- Dempsey, C. E., and Butler, G. S. (1992) *Biochemistry* **31**, 11973–11977
- Halsall, A., and Dempsey, C. E. (1999) *J. Mol. Biol.* **293**, 901–915
- Schwarz, G., and Arbuzaova, A. (1995) *Biochim. Biophys. Acta* **1239**, 51–57
- Matsuzaki, K., Murase, O., Tokuda, H., Funakoshi, S., Fujii, N., and Miyajima, K. (1994) *Biochemistry* **33**, 3342–3349
- Dempsey, C. E., Ueno, S., and Avison, M. B. (2003) *Biochemistry* **42**, 402–409
- Rex, S., and Schwarz, G. (1998) *Biochemistry* **37**, 2336–2345
- Jayalakshmi, V., and Krishna, N. R. (2002) *J. Magn. Reson.* **155**, 106–118
- Bulet, P., Cociancich, S., Reuland, M., Sauber, F., Bischoff, R., Hegy, G., Van Dorsselaer, A., Hetru, C., and Hoffmann, J. A. (1992) *Eur. J. Biochem.* **209**, 977–984
- Maget-Dana, R., and Ptak, M. (1997) *Biophys. J.* **73**, 2527–2533